Advances in Brief

Tea Polyphenol (−)-Epigallocatechin-3-Gallate Inhibits DNA Methyltransferase and Reactivates Methylation-Silenced Genes in Cancer Cell Lines

Ming Zhu Fang,[1] Yimin Wang,[1] Ni Ai,[2] Zhe Hou,[1] Yi Sun,[1] Hong Lu,[1] William Welsh,[2] and Chung S. Yang[1]

[1]*Department of Chemical Biology, Ernest Mario School of Pharmacy, Rutgers, The State University of New Jersey, and* [2]*Department of Pharmacology, Robert Wood Johnson Medical School, University of Medicine and Dentistry of New Jersey, Piscataway, New Jersey*

Abstract

Hypermethylation of CpG islands in the promoter regions is an important mechanism to silence the expression of many important genes in cancer. The hypermethylation status is passed to the daughter cells through the methylation of the newly synthesized DNA strand by 5-cytosine DNA methyltransferase (DNMT). We report herein that (−)-epigallocatechin-3-gallate (EGCG), the major polyphenol from green tea, can inhibit DNMT activity and reactivate methylation-silenced genes in cancer cells. With nuclear extracts as the enzyme source and polydeoxyinosine-deoxycytosine as the substrate, EGCG dose-dependently inhibited DNMT activity, showing competitive inhibition with a K_i of 6.89 μM. Studies with structural analogues of EGCG suggest the importance of D and B ring structures in the inhibitory activity. Molecular modeling studies also support this conclusion, and suggest that EGCG can form hydrogen bonds with Pro^{1223}, Glu^{1265}, Cys^{1225}, Ser^{1229}, and Arg^{1309} in the catalytic pocket of DNMT. Treatment of human esophageal cancer KYSE 510 cells with 5–50 μM of EGCG for 12–144 h caused a concentration- and time-dependent reversal of hypermethylation of $p16^{INK4a}$, retinoic acid receptor β ($RAR\beta$), O^6-methylguanine methyltransferase ($MGMT$), and human *mutL* homologue 1 (*hMLH1*) genes as determined by the appearance of the unmethylation-specific bands in PCR. This was accompanied by the expression of mRNA of these genes as determined by reverse transcription-PCR. The re-expression of $RAR\beta$ and hMLH1 proteins by EGCG was demonstrated by Western blot. Reactivation of some methylation-silenced genes by EGCG was also demonstrated in human colon cancer HT-29 cells, esophageal cancer KYSE 150 cells, and prostate cancer PC3 cells. The results demonstrate for the first time the inhibition of DNA methylation by a commonly consumed dietary constituent and suggest the potential use of EGCG for the prevention or reversal of related gene-silencing in the prevention of carcinogenesis.

Introduction

Green tea is a popular beverage worldwide. It has been shown to prevent carcinogenesis in animal models for different organ sites, and many mechanisms have been proposed for this activity (reviewed in Ref. 1). EGCG[3], the major polyphenol in green tea, has many interesting activities and is believed to be a key active ingredient (1). In previous studies, we have shown that EGCG is methylated by catechol-*O*-methyltransferase to form MeEGCG and DiMeEGCG both *in vitro* and *in vivo* (2, 3). EGCG is also a potent inhibitor of catechol-*O*-methyltransferase activity (3). Catechol-*O*-methyltransferase and DNMT belong to the same superfamily of *S*-adenosylmethionine-dependent methyltransferases. Both enzymes have a common core structure at the catalytic site (4). It is possible that EGCG may also inhibit DNMT by binding to a similar catalytic site.

Hypermethylation of DNA is a key epigenetic mechanism for the silencing of many genes, including those for cell cycle regulation, receptors, DNA repair, and apoptosis (5–8). In this aberrant methylation, the cytosine of the CpG island in or near the promoter region of the newly synthesized DNA strand is methylated by DNMT. The methylated CpG island has higher binding affinity to methyl-CpG binding domain proteins that recruit transcriptional corepressors, such as histone deacetylases and Sin 3A, resulting in chromosome condensation and transcription repression (9, 10). The inhibition of DNMT, especially DNMT1, would block the hypermethylation of the newly synthesized DNA strand, resulting in the reversal of the hypermethylation and the re-expression of the silenced genes (11–13). Indeed, this point has been demonstrated by studies with DNMT inhibitors, DAC (also known as 5-aza-2′-deoxycytidine) and zebularine. These compounds have been shown to inhibit cancer cell growth, induce cancer cell apoptosis, and reduce tumor volume in mice (14–17). There is high potential for developing this group of inhibitors for cancer therapy. However, side effects and toxicity are serious concerns. There is a great need for the development of effective and nontoxic inhibitors of DNMT. We hypothesize that EGCG can be used for this purpose.

In the present study, we tested this hypothesis by examining the inhibition of DNMT by EGCG and the effects of EGCG treatment on four methylation-silenced genes in human esophageal cancer cell line KYSE 510: the tumor suppressor $p16^{INK4a}$, retinoic acid receptor β ($RAR\beta$), O^6-methylguanine methyltransferase ($MGMT$), and the DNA mismatch repair gene human *mutL* homologue 1 (*hMLH1*). In our previous work, these genes have been shown to be frequently silenced by DNA hypermethylation in human esophageal cancer, and some of these genes can be partially reactivated by treatment with the DNMT inhibitor, DAC (18). The results on the inhibition of DNMT and reactivation of methylation-silenced genes by EGCG are reported herein.

Materials and Methods

Cell Lines and Cell Culture. The human esophageal squamous cell carcinoma cell lines KYSE 510 and KYSE 150 were gifts from Dr. Yutaka Shimada (Kyoto University, Kyoto, Japan). The cells were maintained in 5% CO_2 atmosphere at 37°C in RPMI 1640 and Ham F12 mixed (1:1) medium containing 5% fetal bovine serum. To determine the dose-dependent changes, KYSE 510 cells were treated with 5, 10, 20, or 50 μM of EGCG (Unilever-Bestfoods, Englewood Cliffs, NJ) or 8.7 μM of DAC for 6 days. EGCG or DAC was added, in new culture medium, to the cells on days 1, 3, and 5. For the time course study, cells were treated with 20 μM of EGCG for 12, 24, 48, 72, or 144 h. Human colon cancer cell line HT-29 and prostate cancer cell line PC3 were obtained from American Type Culture Collection (Manassas, VA), and were grown in McCoy's 5A and RPMI 1640 containing 10% fetal bovine

Table 1 *List of primers, annealing temperatures, and product sizes for methylation-specific PCR and RT-PCR*

Gene	Chromosome location	Forward primer (5′–3′)	Reverse primer (5′–3′)	Annealing temperature (°C)	Product size (bp)
Methylation-specific PCR[a]					
RARβ	*3p24*	N: TTAAG(C/T)TTTGTGAGAATTTTG	CCTATAATTAATCCAAATAATCATTTA CC	53	425
		U: TTGAGAATGTGAGTGATTTGA	AACCAATCCAACCAAAACAA	62	146
		M: TCGAGAACGCGAGCGATTCG	GACCAATCCAACCGAAACGA	62	146
MGMT	*10q26*	N: GGATATGTTG GGATAGTT	CCAAAAACCCCAAACCC	52	289
		U: TTTGTGTTTTGATGTTTGTAGGTTTTTGT	AACTCCACACTCTTCCAAAAACAAAACA	59	93
		M: TTTCGACGTTCGTAGGTTTTCGC	GCACTCTTCCGAAAACGAAACG	59	81
P16	*9p21*	N: GGAGAGGGGGAGAGTAGGT	CTACAAACCCTCTACCCACCT	60	208
		U: TGGGGAGTAGTATGGAGTTGGTGGT	CAACCCCAAACCACAACCATAA	62	81
		M: CGGGGAGTAGTATGGAGTCGGCGGC	GACCCCGAACCGCGACCGTAA	62	81
hMLH1	*3p22*	N: GGTATTTTTGTTTTTATTGGTTGGAT	AATACCAATCAAATTTCTCAACTCCT	55	185
		U: TAAAAATGAATTAATAGGAAGAGT	CTCTATAAATTACTAAATCTCTTCA	60	117
		M: TAAAAACGAATTAATAGGAAGAGC	CTCTATAAATTACTAAATCTCTTCG	60	117
RT-PCR					
RARβ		GACTGTATGGATGTTCTGTCAG	ATTTGTCCTGGCAGACGAAGCA	60	256
MGMT		AAAATGGACAAGGATTGTGAAA	CATCCGATGCAGTGTTACACG	57	568
P16		CGGAAGGTCCCTCAGACATC	TCATGAAGTCGACAGCTTCCG	60	385
hMLH1		CAGCGGCCAGCTAATGCTAT	AATCCTCAAAGGACTGCAGTT	60	195
DNMT1		ACCAAGCAAGAAGTGAAGCC	GCTTCCTGCAGAAGAACCTG	60	336
DNMT3a		CACACAGAAGCATATCCAGGAGTG	AGTGGAAACCAAATACCC	60	550
DNMT3b		AATGTGAATCCAGCCAGGAAAGGC	ACTGGATTACACTCCAGGAACCGT	60	191
MBD2		AACCCTGCTGTTTGGCTTAAC	CGTACTTGCTGTACTCGCTCTTC	60	101
G3DPH		TTGCAACTGTTTTAGGACTTT	AGCATTGGGAAATGTTCAAGG	60	983

[a] N, nest primers; U, unmethylation-specific primers; and M, methylation-specific primers.

serum, respectively. These cells were treated with EGCG for 6 days as described above.

DNA Methyltransferase Assay. Cultured KYSE 510 cells were harvested, and nuclear extracts were prepared with the nuclear extraction reagent (Pierce, Rockford, IL). The DNMT assay was performed according to published methods (19, 20). In brief, the nuclear extracts (4 μg of protein) were incubated for 1.5 or 2 h at 37°C with 0.66 μM of poly(dI-dC)·poly(dI-dC) and 10 μM of *S*-adenosyl-L-[methyl-³H]methionine (2 μCi; Amersham, Piscataway, NJ) in a total volume of 40 μl of a pH 7.4 buffer, containing 20 mM Tris-HCl, 25% glycerol (v/v), 10 mM EDTA, 0.2 mM phenylmethylsulfonyl fluoride, and 20 mM 2-mercaptoethanol. All of the incubations contained 0.02% DMSO, which was used to dissolve EGCG and other inhibitors. Reactions were initiated by the addition of nuclear extracts and stopped by mixing with 300 μl of a solution containing 1% SDS, 3% 4-aminosalicylate, 5% butanol, 2.0 mM EDTA, 125 mM NaCl, 0.25 mg/ml carrier salmon testes DNA (Life Technologies, Inc., Gaithersburg, MD), and 1 mg/ml protease K (Sigma, St. Louis, MO). To remove proteins, the resulting mixture was vortexed with 300 μl of a solution containing 8% phenol, 12% m-cresol, and 0.1% 8-hydroxyquinoline (Sigma), and centrifuged. The methylated DNA template was recovered from the aqueous phase by ethanol precipitation and then washed three times with 70% ethanol. The radioactivity in the pellets was counted in a scintillation counter. All of the assays were performed in duplicate. Background levels were determined in incubations without the template DNA.

***In Silico* Molecular Modeling Studies of DNMT1.** The protein sequence of DNMT1 (accession no. NP_001370) was retrieved from the National Center for Biotechnology Information Reference Sequence (RefSeq) Collection. A structural model of the catalytic domain of DNMT1 was constructed using the Insight II Homology Module (Accelrys, Inc., San Diego, CA) from the published crystal structure of *Hha*I Mtase (RCSB Protein Data Bank;[4] PDB ID = 5MHT) as the modeling template. The quality of the model was confirmed by the WHATIF-Check program.[5] Initial structures of EGCG and the five analogues were built using the Insight II Builder Module and subsequently energy minimized to yield a stable conformation. Each ligand was docked into the putative DNMT1 binding pocket using GOLD (Genetic Optimization for Ligand Docking; Ref. 21), which accommodates ligand flexibility and partial enzyme flexibility to satisfy ligand-enzyme binding requirements. After these docking studies to elucidate stable ligand-binding modes, values of the ligand-enzyme binding energy ($\Delta E_{binding}$) were calculated

for each of the six ligands using molecular mechanics procedures. Residues within 5.0 Å of the cytosine nucleotide were defined as the "active site" pocket and were permitted full relaxation, while holding all of the other residues fixed. We define $\Delta E_{binding}$ as the difference between the potential energy of the ligand-enzyme ($E_{complex}$) and the sum of potential energies of the ligand (E_{ligand}) and enzyme (E_{enzyme}).

$$\Delta E_{binding} = E_{complex} - (E_{ligand} + E_{enzyme})$$

A favorable (more negative) binding energy is taken as evidence that the ligand possesses high affinity for DNMT1.

Bisulfite Modification and Methylation-Specific PCR. DNA was extracted from the cells using the DNeasy tissue kit (Qiagen, Valencia, CA), and was denatured with 0.2 M NaOH at 37°C for 30 min. The denatured DNA was treated with 3.3 M sodium bisulfite and 0.66 mM hydroquinone according to Herman *et al.* (22), with slight modifications (18). The modified DNA was purified using the Qiaquick gel extraction kit (Qiagen) and eluted with water. NaOH was added to the modified DNA for a final concentration of 0.3 M and maintained for 5 min at room temperature to desulfonate the modified DNA. The resulting DNA was repurified with Qiaquick gel and used immediately or stored at −20°C.

Methylation-specific PCR was carried out using a nested two-stage PCR approach (23). Stage I PCR was performed on bisulfite-modified DNA to amplify a 208-, 289-, 425-, or 185-bp fragment of the CpG-rich promoter regions of the *p16^{INK4a}, MGMT, RARβ,* or *hMLH1* genes, respectively. The primers recognize the bisulfite-modified template but do not discriminate between methylated and unmethylated alleles. The stage I PCR products were diluted and subjected to a stage II PCR with primer sets specific to methylated or unmethylated template. The primers were designed according to the literature (23–27). The chromosomal locations of all of the genes tested, primer sequences for both the methylated and unmethylated templates, annealing temperatures used, and expected PCR product sizes are summarized in Table 1. Placental DNA and placental DNA treated with *Sss*I methyltransferase (New England Biolabs, Beverly, MA) were used as positive controls for unmethylated alleles and methylated alleles, respectively. Amplification was carried out using a 9700 Perkin-Elmer thermal cycler (Applied Biosystems, Foster City, CA).

Reverse Transcription-PCR. Total RNA was isolated from cells by the Tri reagent (Sigma). Reverse transcription of RNA was performed using the Advantage RT-for-PCR kit (Clontech, Palo Alto, CA). PCR was carried out using a 9700 Perkin-Elmer thermal cycler. The primers used in the PCR

---

[4] Internet address: http://www.rcsb.org/pdb.
[5] Internet address: http://www.cmbi.kun.nl/gv/servers/WIWWWI.

reactions for the genes analyzed (13, 28, 29) are summarized in Table 1. The PCR reactions were run in an approximate linear range (for example, 25–28 cycles for *p16^INK4a*, 30–35 cycles for *RARβ*, 20–25 cycles for *hMLH1*, and 30–35 cycles for *MGMT*). The amplified products were subjected to electrophoresis on a 2% agarose gel. The gel was then stained with ethidium bromide and photographed. Negative controls for PCR were run under the same conditions without RNA or reverse transcriptase. Expression of the glyceraldehyde-3-phosphate dehydrogenase gene (*G3PDH*) was used to examine the integrity of RNA in each sample and to standardize the amount of cDNA added to each of the PCR reactions.

Western Blot. The protein samples in SDS-containing lysis buffer were loaded on 4–15% acrylamide gel (40 μg/lane). After electrophoresis, the proteins were blotted onto a nitrocellulose membrane. After incubation in blocking buffer (5% nonfat milk), the membranes were incubated with the primary antibodies (rabbit antihuman RARβ and hMLH1 polyclonal antibodies; Santa Cruz Biotechnology, Santa Cruz, CA) overnight at 4°C. After washing with Tris-buffered saline containing 0.1% Tween 20, the membrane was then incubated with sheep antirabbit horseradish peroxidase-labeled secondary antibody and visualized using the electrochemiluminescense detection kit (Amersham).

Results

Inhibition of DNA Methyltransferase Activity by EGCG. With nuclear extracts from the KYSE 510 cells as the enzyme source and poly(dI-dC)·poly(dI-dC) as the substrates for DNMT, under our assay conditions, the production of methylated poly(dI-dC)·poly(dI-dC) was linear for 2 h. A dose-dependent inhibition by EGCG was observed, with an IC$_{50}$ of ~20 μM (Fig. 1*A*). The structural analogues of EGCG: ECG, EGC, EC, and methylated EGCG all had inhibitory activities, with potency in the rank order of EGCG > ECG, MeEGCG > EGC, and DiMeEGCG > EC. Kinetic studies indicated that EGCG increases the K_m of DNMT without affecting the V_{max}, suggesting a competitive inhibition with a K_i of 6.89 μM (Fig. 1*B*). The same conclusion was reached when this experiment was repeated.

Molecular Modeling of the Interaction between EGCG and DNMT. To investigate the possible inhibition mechanism of EGCG to DNMT1, we used information available from the X-ray crystal structure of *Hha*I Mtase (30) to model the three-dimensional structure of the DNMT1 catalytic domain. This structural model revealed a substantial interaction region with hemimethylated DNA and a cytosine active pocket for subsequent methylation, which was folded by evolutionarily conserved sequence motifs identified from multiple sequence alignments (Fig. 2*A*). Docking of EGCG into the putative cytosine pocket indicated that the gallate moiety of this compound formed potential hydrogen bonds with two catalytically important residues, Glu^{1265} and Pro^{1223}, which were the same residues that appear to stabilize the flipped cytosine through hydrogen bonding. Interestingly, the D ring was oriented at approximately the same position as the pyrimidyl ring of cytosine in the structural model of DNMT1. Furthermore, Ser^{1229} and Cys^{1225} are positioned to form hydrogen bonds with the hydroxy groups in the A and B rings of EGCG, respectively, thereby contributing to high-affinity DNMT1 binding. The interactions are depicted in Fig. 2*B*. These findings suggest that EGCG exerts its inhibitory effect on DNMT1 function by blocking entry of the key nucleotide cytosine into its active site and, thus, prevents methylation. A consensus-binding mode was obtained from 25 independent docking procedures for EGCG and each of the five analogues bound to DNMT1. Accordingly, calculated values of Δ E$_{binding}$ (shown in parentheses, in units of kcal/mol) for each ligand in its consensus-binding mode yielded the following order of binding affinity to DNMT1: EGCG (−49.75) > ECG (−46.53)> Me-EGCG (−44.91) > diMe-EGCG (−41.64) > EGC (−40.79) > EC
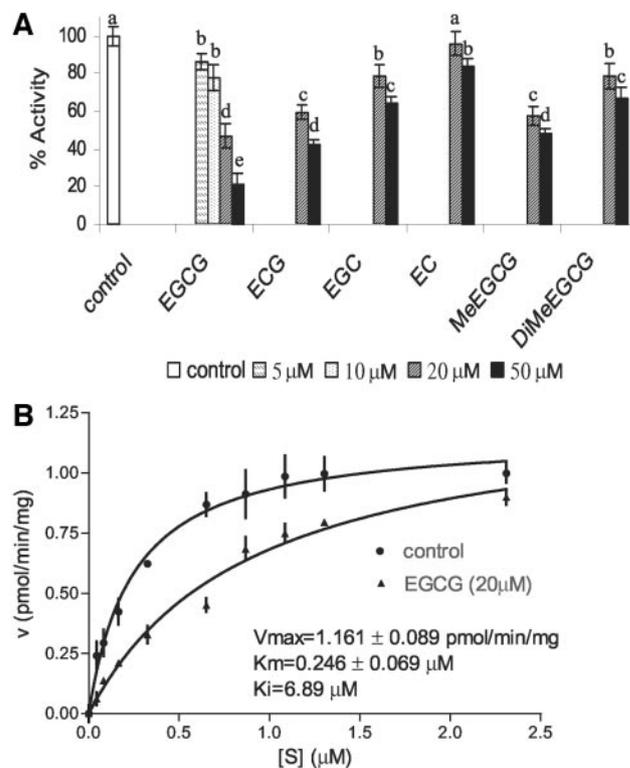

Fig. 1. Inhibition of 5-cytosine DNA methyltransferase activity by EGCG. *A,* inhibition of DNMT by different concentrations of EGCG and 20 or 50 μM of other compounds. The reaction mixture contained nuclear extracts (4 μg protein), poly(dI-dC)·poly(dI-dC; 0.66 μM), and *S*-adenosyl-L-[methyl-^{3}H]methionine (10μM, 2.0 μCi) in 40 μl. The incubation time was 2 h. The results are mean of 6–10 determinations, and are analyzed by one-way ANOVA (SigmaStat 1.01) using Student-Newman-Keuls pairwise test; *bars,* ±SD. *Bars identified by different letters* signified that they are significantly different (*P* < 0.05). *B,* kinetic studies on the inhibition of DNMT by EGCG. The reaction mixture contained 10 μM of *S*-adenosyl-L-[methyl-^{3}H]methionine, and different concentrations of poly(dI-dC)·poly(dI-dC), and was incubated for 1.5 h. Each *data point* represents the mean ± SD of 4 determinations, and the data were analyzed by GraphPad Prism 4. In the absence of EGCG, the mean ± 95% confidence interval of the V_{max} was 1.161 ± 0.089 pmol/min/mg and of the K_m was 0.246 ± 0.070 μM. In the presence of 20 μM EGCG, the V_{max} was 1.235 ± 0.205 pmol/min/mg, and K_m was 0.897 ± 0.210 μM, showing a competitive inhibition with a K_i of 6.89 μM.

(−38.32). These predicted results are generally consistent with the experimental data.

Reversal of Hypermethylation and Reactivation of *RARβ*, *MGMT*, *p16^INK4a*, and *hMLH1* by EGCG. In KYSE 510 cells, *p16^INK4a*, *RARβ*, *MGMT*, and *hMLH1* had hypermethylation status with the loss of the respective mRNA expression. After treating the cells with 5, 10, 20, or 50 μM of EGCG for 6 days, the methylation-specific bands of these four genes still existed. The unmethylation-specific bands of these four genes, however, appeared after treatment with 20 or 50 μM of EGCG for 6 days (Fig. 3*A*). Corresponding to the appearance of the unmethylation-specific band was the re-expression of mRNA of all four of the genes. The unmethylation-specific bands and mRNA expression were both observed with 20 and 50 μM of EGCG. For *hMLH1*, the unmethylation-specific band was observed even with 10 μM of EGCG in comparison to the faint bands observed with 0 and 5 μM EGCG (Fig. 3*A*). The reversal of hypermethylation and re-expression of these four genes by EGCG was similar to that produced by the classical DNMT inhibitor, DAC. After treating the cells with 20 μM of EGCG for 0, 12, 24, 48, 72, and 144 h, strong unmethylation-specific bands for all four of the genes began to appear at 48 h (Fig. 3*A*). The mRNA expression of these four genes was also observed at 48 h and, depending on the genes, higher levels were observed at either 72 or 144 h. Again, a faint *hMLH1* mRNA band
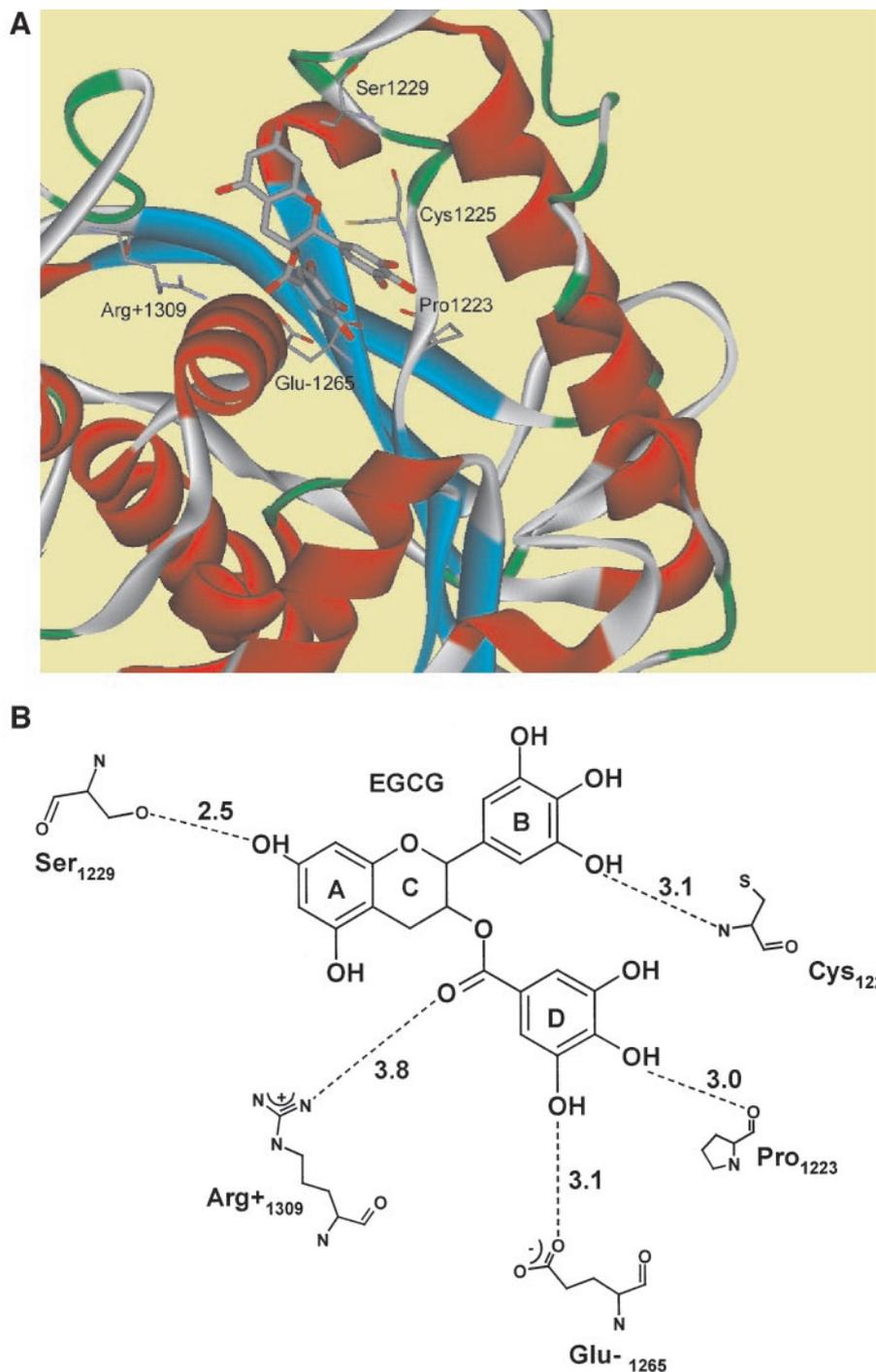
Fig. 2. Molecular modeling of the interaction between EGCG and DNMT. *A,* binding orientation of EGCG in DNMT1. The close-up view of the consensus orientation for EGCG. The protein is depicted in ribbon representation and colored by secondary structures (*i.e.,* helix, strand, and loop). Both EGCG and ligand contact residues are represented in stick form and colored by atom type with carbon in *gray,* oxygen in *red,* and sulfur in *yellow*. *B,* hydrogen-binding network of EGCG in DNMT1. ---- represents hydrogen bond. Figure depicts all potential H-bonding X-H. . . Y interactions for which the X. . . Y distance is <4.0 Å.

was observed at 0, 12, and 24 h. Similar results were obtained in two repeated experiments.

Using the reactivation of *RARβ* mRNA as an assay, ECG was found to be slightly less active than EGCG; EGC, MeEGCG, and EC had lower activities than EGCG; and DiMeEGCG had no activity when the cells were treated with 20 μM of the test agents for 6 days (Fig. 3*B*). In another experiment, demethylation and reactivation of *RARβ* was observed with DiMeEGCG at 50 μM, but not at 20 μM (data not shown).

Western blot analysis indicated that the RARβ protein expression was increased in the cells treated with 20 and 50 μM of EGCG for 6 days (Fig. 4). A time-dependent increase of hMLH1 protein expression level was observed in the cells treated with 20 μM of EGCG for

3 and 6 days. Because of the lack of suitable antibodies, we were unable to accurately analyze the re-expression of MGMT and p16^{INK4a} proteins.

To determine whether the reactivation of methylation-silenced genes by EGCG is a general phenomenon that also occurs in other cell lines, we studied the effects of EGCG treatment on the methylation status and mRNA levels of *p16^{INK4a}* or *RARβ* in three other human cancer cell lines (Fig. 3*C*). The appearance of unmethylation-specific bands and reactivation of the mRNA of *p16^{INK4a}* in HT-29 cells, and *RARβ* in KYSE 150 and PC3 cells, were observed after treating the cells with 20 μM EGCG for 6 days. In the KYSE 150 cells, a faint *RARβ* mRNA band was also observed in cells without EGCG treatment, but the band was much
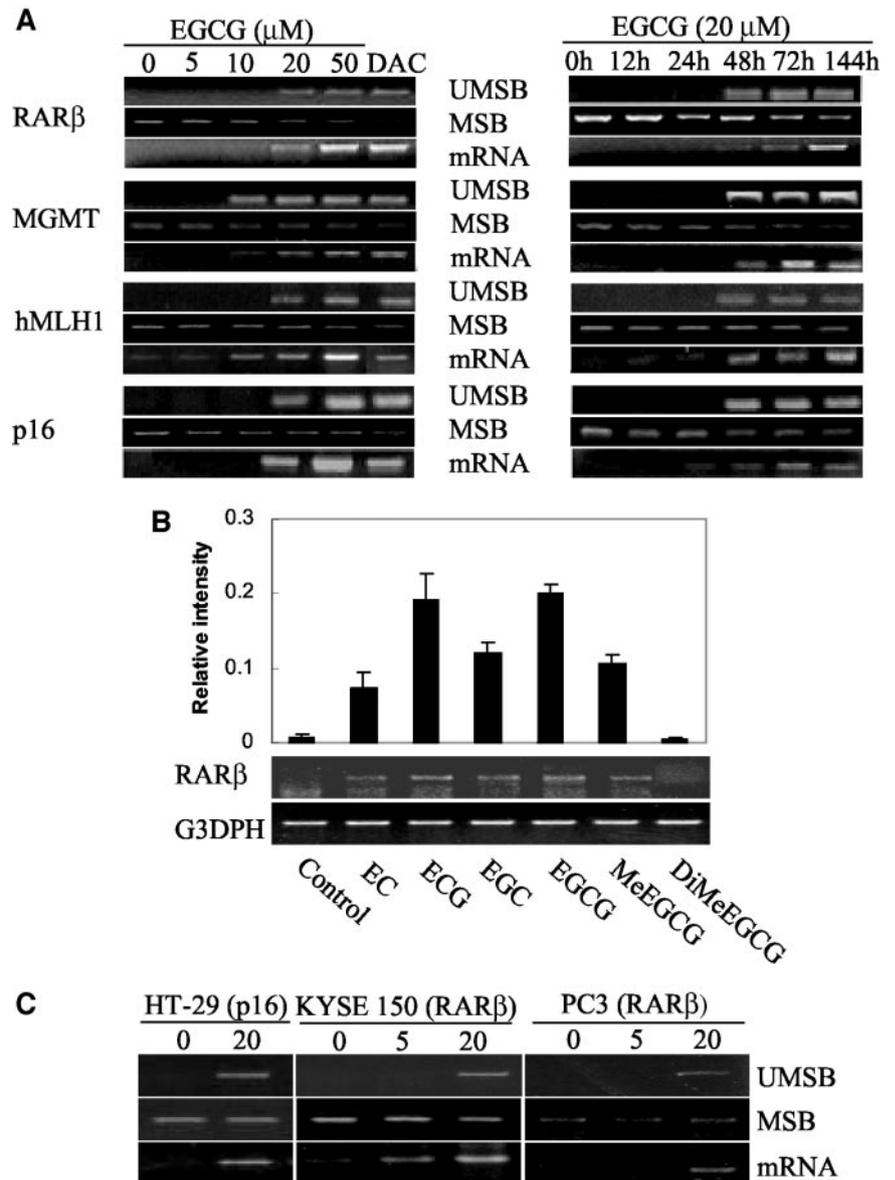
A

B

C

Fig. 3. Alterations of methylation status and mRNA expression levels of *RARβ, MGMT, p16,* or *hMLH1* genes after treatment with EGCG or other polyphenols. For each gene, the *top panel* presents the unmethylation-specific bands (*UMSB*), the *middle panel* presents the methylation-specific bands (*MSB*), and the *bottom panel* presents the mRNA expression levels (*mRNA*). *A, left:* KYSE 510 cells were treated with 5, 10, 20, or 50 μM of EGCG or 8.7 μM of DAC for 6 days as described in "Materials and Methods;" *right:* the cells were treated for 12, 24, 48, 72, and 144 h with 20 μM of EGCG added in new culture medium at 0, 48, and 96 h. *B, RARβ* mRNA levels of KYSE 510 cells treated with 20 μM of different polyphenols for 6 days. The *RARβ* mRNA level was determined with RT-PCR with *G3DPH* as an internal control. The band intensity was determined with densitometry. The values presented are mean ($n = 3$); bars, $\pm$SD. *C,* HT-29, KYSE150, and PC3 cells were treated with 5 or 20 μM of EGCG for 6 days under conditions described in "Materials and Methods."

more intense after EGCG treatment. These results were reproduced in three experiments with the three cell lines. The results, although still preliminary in a quantitative sense, demonstrate that the reactivation of methylation-silenced genes does occur in different cell lines, suggesting it is a general phenomenon.

Inhibition of Cell Growth and Other Effects. After treatment with EGCG for 6 days, significant inhibition of cell growth was not observed at 5 or 10 μM, but 36 and 54% inhibition were observed at 20 and 50 μM of EGCG, respectively (Fig. 5A). Many damaged cells and some polynuclear cells were observed with 50 μM of EGCG, and to a lesser extent with 20 μM of EGCG, in this 6-day experiment (Fig. 5C). In experiments in which cells were treated for 2 days with EGCG, growth inhibition and signs of toxicity were not apparent at 5, 10, or 20 μM; but at 50 μM, some damaged cells with vesicles were observed (Fig. 5C). After treatment of the cells with 50 μM of EGCG for 2 days, the colony formation (measured after an additional 7 days of culturing) was inhibited by 55%, but significant inhibition was not observed with EGCG at 20 μM or lower concentrations (Fig. 5B). Preliminary experiments with RT-PCR also indicated that EGCG treatment did not affect the mRNA expression level of DNMT1, DNMT3a, DNMT3b, and MBD2 (methyl-CpG binding domain protein 2), which has been reported to have DNA demethylase activity (31).

Discussion

The present study clearly demonstrates that EGCG inhibits DNMT activity, and causes CpG demethylation and reactivation of methylation-silenced genes. To our knowledge, this is the first demonstration of such an activity of a commonly consumed dietary constituent. Kinetic studies indicate that EGCG inhibits nuclear DNMT activity competitively with a K_i of 6.89 μM. We believe that most of the activity is because of the dominant form of DNMT, DNMT1, although DNMT 3a and 3b may also be present in smaller quantities in the nuclear extracts (14). Molecular modeling studies indicate that EGCG is well accommodated in a hydrophilic pocket of DNMT1. As depicted in Fig. 2B, EGCG is effectively tethered within the DNMT1 binding site by at least four hydrogen bonds involving Ser[1229] (2.5Å), Glu[1265] (3.1Å), Pro[1223] (3.0 Å), and Cys[1225] (3.1Å). An additional hydrogen bond is possible with the protonated side chain of Arg[1309], although the N. . . O distance (3.8Å) is at the outer limit of the typical hydrogen bond and, thus,
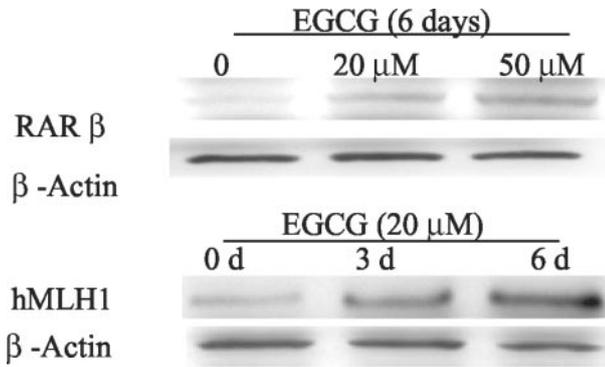
Fig. 4. Re-expression of RARβ and hMLH1 proteins after EGCG treatment. KYSE 510 cells were treated with 20 and 50 μM EGCG for 6 days, or 20 μM for 3 and 6 days; protein levels were determined with Western blot analysis using β-actin as an internal control.

would imply a weak interaction. This hydrogen-bonding scheme is consistent with the observed reduction in DNMT1 inhibitory activity for the five EGCG structural analogues. The absence of the B-ring 3′-hydroxy group in ECG abolishes the hydrogen bond with Cys[1225]. Likewise, the absence of the 4″-hydroxy group in MeEGCG eliminates the hydrogen bond with Pro[1223]. Addition of another methyl group at the B ring as in DiMeEGCG additionally interferes with the binding. The importance of galloyl moiety in EGCG-like compounds is evident from interactions with the two conserved residues, Glu[1265] and Pro[1223], which are associated with the catalytic activity of DNMT1. This observation concurs with the experimental results for EGC and EC, two poor DNMT1 inhibitors in which the galloyl moiety is conspicuously absent.

The activities of these compounds to reactivate RARβ mRNA expression are also correlated with their ability to inhibit DNMT activity. With EGCG, demethylation and reactivation of all four of the genes are observable after 48 h of treatment, and 20 μM is the effective concentration that activates all four of the genes. All of the results are consistent with our hypothesis that reactivation of methylation-silenced genes is due to the inhibition of DNMT by EGCG. More work is needed to determine the quantitative reactivation of the different genes as well as the extents of the demethylation in different cell lines under different treatment conditions. It would be interesting to determine whether the different hypermethylated genes respond similarly or differently to the EGCG treatment. The reactivated p16[INK4a] is expected to regain its function in cell cycle regulation, and re-expressing RARβ is expected to regain responsiveness to retinoic acids. It is not clear whether the presently observed growth-inhibitory effect after 2 or 6 days of treatment with EGCG are related to the reactivation of these genes. The functional importance of the reactivation of those genes remains to be determined.

Hypermethylation of DNA is a key epigenetic mechanism for the silencing of many genes including those for tumor suppressors, DNA repair enzymes, and receptors (5–8). In theory, this epigenetic process is reversible if the newly synthesized DNA strands are not methylated. Therefore, DNMT inhibitors such as DAC and zebularine have been actively explored as cancer therapeutic agents, especially when they are used in combination with a
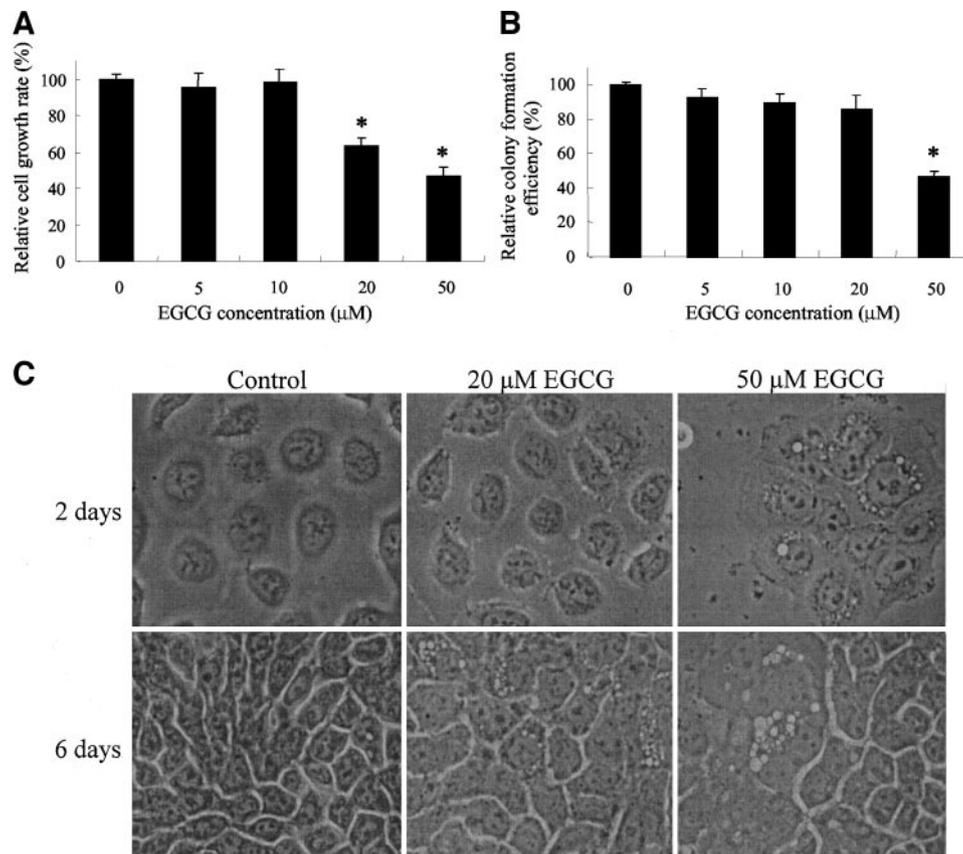

Fig. 5. Effects of EGCG treatment on cell growth, colony formation, and morphological change. A, KYSE 510 cells were treated with EGCG, and after 6 days, its effect on cell growth was determined by counting living cell numbers by the trypan blue exclusion assay. B, after the cells were treated with EGCG for 2 days, the cells were washed, cultured with new medium (without EGCG) for another 7 days, and colony number was analyzed. C, morphological changes (magnification, ×400) after 2 and 6 days of EGCG treatment are shown. The values presented are mean (n = 3); bars, ±SD. * indicates statistically significant (P < 0.05).

histone deacetylase inhibitor, such as trichostatin A (15, 26, 32–36). It has also been suggested that methylation is not the initial event in triggering gene silencing in cancer; rather, the methylation of the promoter CpG islands is a consequence of prior gene inactivation, and it is a mechanism for locking the chromatin in a repressed state (5, 13, 37). Many tumor suppressor and receptor genes have been reported to be hypermethylated and transcriptionally silenced during the development of different types of cancers. It is likely that inhibition of DNMT and histone deacetylase can also prevent the hypermethylation and silencing of these key genes and, therefore, this inhibition would contribute to the prevention of carcinogenesis. The prevention of intestinal tumorigenesis by *Dnmt1* deficiency and by DAC has been demonstrated in the *Min* mice, which carry a mutated *Apc* gene (38, 39).

Oral administration of green tea has been shown to inhibit tumorigenesis in different organs, and multiple mechanisms may be involved (1). It remains to be determined whether and to what extent this cancer-preventive activity is due to the inhibition of DNMT by EGCG. The presently observed effective dose of EGCG, Ki of 6.89 μM, or IC$_{50}$ of 20 μM, is achievable in the oral cavity (in the saliva) after drinking green tea, and perhaps in the stomach, esophagus, and intestines where there is direct contact between EGCG and the epithelial cells. This effective concentration, however, is higher than those in the internal organs, which depend on the systemic bioavailability of EGCG (1). Therefore, the extent of DNMT inhibition *in vivo* would depend on the bioavailability of EGCG in a particular organ site. Although inhibition of DNMT is expected to prevent hypermethylation, severe inhibition of DNMT activity, as suggested by recent genetic studies, may cause DNA hypomethylation, genomic instability, and early development of cancers such as T-cell lymphomas and sarcomas (40, 41). There is no evidence for such adverse effects due to regular consumption of tea; however, it could be a concern if large doses of EGCG are given to humans.

On the basis of this analysis, for the practical application of tea in the prevention of cancer, it may be desirable to use doses to produce levels of EGCG in the tissue that would cause a moderate inhibition of DNMT. The possible synergy generated between EGCG with histone deacetylase inhibitors or other agents will hold great promise. For example, butyrate, which is a histone deacetylase inhibitor produced in the colon (42), may work synergistically with EGCG in the prevention of colon cancer. The application of this concept in animal models or humans remains to be demonstrated.

Acknowledgments

References

1. Yang, C. S., Maliakal, P., and Meng, X. Inhibition of carcinogenesis by tea. Annu. Rev. Pharmacol. Toxicol., *42:* 25–54, 2002.
2. Meng, X., Sang, S., Zhu, N., Lu, H., Sheng, S., Lee, M. J., Ho, C. T., and Yang, C. S. Identification and characterization of methylated and ring-fission metabolites of tea catechins formed in humans, mice, and rats. Chem. Res. Toxicol., *15:* 1042–1050, 2002.
3. Lu, H., Meng, X., Li, C., Sang, S., Patten, C., Sheng, S., Hong, J., Bai, N., Winnik, B., Ho, C. T., and Yang, C. S. Glucuronides of tea catechins: enzymology of biosynthesis and biological activities. Drug Metab. Dispos., *31:* 452–461, 2003.
4. Cheng, X. Structure and function of DNA methyltransferases. Annu. Rev. Biophys. Biomol. Struct., *24:* 293–318, 1995.
5. Esteller, M. CpG island hypermethylation and tumor suppressor genes: a booming present, a brighter future. Oncogene, *21:* 5427–5440, 2002.
6. Jones, P. A., and Baylin, S. B. The fundamental role of epigenetic events in cancer. Nat. Rev. Genet., *3:* 415–428, 2002.
7. Jones, P. A., and Takai, D. The role of DNA methylation in mammalian epigenetics. Science (Wash. DC), *293:* 1068–1070, 2001.
8. Lichtenstein, A. V., and Kisseljova, N. P. DNA methylation and carcinogenesis. Biochemistry (Mosc.), *66:* 235–255, 2001.
9. Nguyen, C. T., Gonzales, F. A., and Jones, P. A. Altered chromatin structure associated with methylation-induced gene silencing in cancer cells: correlation of accessibility, methylation, MeCP2 binding and acetylation. Nucleic Acids Res., *29:* 4598–4606, 2001.
10. Rice, J. C., Massey-Brown, K. S., and Futscher, B. W. Aberrant methylation of the BRCA1 CpG island promoter is associated with decreased BRCA1 mRNA in sporadic breast cancer cells. Oncogene, *17:* 1807–1812, 1998.
11. Robertson, K. D., Ait-Si-Ali, S., Yokochi, T., Wade, P. A., Jones, P. L., and Wolffe, A. P. DNMT1 forms a complex with Rb, E2F1 and HDAC1 and represses transcription from E2F-responsive promoters. Nat. Genet., *25:* 338–342, 2000.
12. Rountree, M. R., Bachman, K. E., and Baylin, S. B. DNMT1 binds HDAC2 and a new co-repressor, DMAP1, to form a complex at replication foci. Nat. Genet., *25:* 269–277, 2000.
13. Clark, S. J., and Melki, J. DNA methylation and gene silencing in cancer: which is the guilty party? Oncogene, *21:* 5380–5387, 2002.
14. Christman, J. K. 5-Azacytidine and 5-aza-2′-deoxycytidine as inhibitors of DNA methylation: mechanistic studies and their implications for cancer therapy. Oncogene, *21:* 5483–5495, 2002.
15. Zhou, L., Cheng, X., Connolly, B. A., Dickman, M. J., Hurd, P. J., and Hornby, D. P. Zebularine: a novel DNA methylation inhibitor that forms a covalent complex with DNA methyltransferases. J. Mol. Biol., *321:* 591–599, 2002.
16. Cheng, J. C., Matsen, C. B., Gonzales, F. A., Ye, W., Greer, S., Marquez, V. E., Jones, P. A., and Selker, E. U. Inhibition of DNA methylation and reactivation of silenced genes by zebularine. J. Natl. Cancer Inst., *95:* 399–409, 2003.
17. Bender, C. M., Pao, M. M., and Jones, P. A. Inhibition of DNA methylation by 5-aza-2′-deoxycytidine suppresses the growth of human tumor cell lines. Cancer Res., *58:* 95–101, 1998.
18. Wang, Y., Fang, N. Z., Liao, J., Yang, G-Y., Nie, Y., Song, Y., So, C., Xu, X., Wang, L-D., and Yang C. S. Hypermethylation associated inactivation of retinoic acid receptor β (RARβ) in human esophageal squamous cell carcinoma. Clin. Cancer Res., in press, 2003.
19. Belinsky, S. A., Nikula, K. J., Baylin, S. B., and Issa, J. P. Increased cytosine DNA-methyltransferase activity is target-cell-specific and an early event in lung cancer. Proc. Natl. Acad. Sci. USA, *93:* 4045–4050, 1996.
20. Adams, R. L., Rinaldi, A., and Seivwright, C. Microassay for DNA methyltransferase. J Biochem Biophys Methods, *22:* 19–22, 1991.
21. Jones, G., Willett, P., Glen, R. C., Leach, A. R., and Taylor, R. Development and validation of a genetic algorithm for flexible docking. J. Mol. Biol., *267:* 727–748, 1997.
22. Herman, J. G., Graff, J. R., Myohanen, S., Nelkin, B. D., and Baylin, S. B. Methylation-specific PCR: a novel PCR assay for methylation status of CpG islands. Proc. Natl. Acad. Sci. USA, *93:* 9821–9826, 1996.
23. Palmisano, W. A., Divine, K. K., Saccomanno, G., Gilliland, F. D., Baylin, S. B., Herman, J. G., and Belinsky, S. A. Predicting lung cancer by detecting aberrant promoter methylation in sputum. Cancer Res., *60:* 5954–5958, 2000.
24. Kresty, L. A., Mallery, S. R., Knobloch, T. J., Song, H., Lloyd, M., Casto, B. C., and Weghorst, C. M. Alterations of p16(INK4a) and p14(ARF) in patients with severe oral epithelial dysplasia. Cancer Res., *62:* 5295–5300, 2002.
25. Esteller, M., Hamilton, S. R., Burger, P. C., Baylin, S. B., and Herman, J. G. Inactivation of the DNA repair gene O6-methylguanine-DNA methyltransferase by promoter hypermethylation is a common event in primary human neoplasia. Cancer Res., *59:* 793–797, 1999.
26. Bovenzi, V., and Momparler, R. L. Antineoplastic action of 5-aza-2′-deoxycytidine and histone deacetylase inhibitor and their effect on the expression of retinoic acid receptor β and estrogen receptor α genes in breast carcinoma cells. Cancer Chemother. Pharmacol., *48:* 71–76, 2001.
27. Murata, H., Khattar, N. H., Kang, Y., Gu, L., and Li, G. M. Genetic and epigenetic modification of mismatch repair genes hMSH2 and hMLH1 in sporadic breast cancer with microsatellite instability. Oncogene, *21:* 5696–5703, 2002.
28. Ng, M. H., Chung, Y. F., Lo, K. W., Wickham, N. W., Lee, J. C., and Huang, D. P. Frequent hypermethylation of p16 and p15 genes in multiple myeloma. Blood, *89:* 2500–2506, 1997.
29. Margison, G. P., Santibanez Koref, M. F., and Povey, A. C. Mechanisms of carcinogenicity/chemotherapy by O^6-methylguanine. Mutagenesis, *17:* 483–487, 2002.
30. O'Gara, M., Klimasauskas, S., Roberts, R. J., and Cheng, X. Enzymatic C5-cytosine methylation of DNA: mechanistic implications of new crystal structures for HhaI methyltransferase-DNA-AdoHcy complexes. J. Mol. Biol., *261:* 634–645, 1996.
31. Detich, N., Theberge, J., and Szyf, M. Promoter-specific activation and demethylation by MBD2/demethylase. J. Biol. Chem., *277:* 35791–35794, 2002.
32. Aparicio, A., Eads, C. A., Leong, L. A., Laird, P. W., Newman, E. M., Synold, T. W., Baker, S. D., Zhao, M., and Weber, J. S. Phase I trial of continuous infusion 5-aza-2′-deoxycytidine. Cancer Chemother. Pharmacol., *51:* 231–239, 2003.
33. Shi, H., Wei, S. H., Leu, Y. W., Rahmatpanah, F., Liu, J. C., Yan, P. S., Nephew, K. P., and Huang, T. H. Triple analysis of the cancer epigenome: an integrated microarray system for assessing gene expression, DNA methylation, and histone acetylation. Cancer Res., *63:* 2164–2171, 2003.
34. Saunders, N., Dicker, A., Popa, C., Jones, S., and Dahler, A. Histone deacetylase inhibitors as potential anti-skin cancer agents. Cancer Res., *59:* 399–404, 1999.
35. Shaker, S., Bernstein, M., Momparler, L. F., and Momparler, R. L. Preclinical evaluation of antineoplastic activity of inhibitors of DNA methylation (5-aza-2′-

deoxycytidine) and histone deacetylation (trichostatin A, depsipeptide) in combination against myeloid leukemic cells. Leuk. Res., *27:* 437–444, 2003.

36. Yoshida, M., Furumai, R., Nishiyama, M., Komatsu, Y., Nishino, N., and Horinouchi, S. Histone deacetylase as a new target for cancer chemotherapy. Cancer Chemother. Pharmacol., *48*(Suppl. 1)*:* S20–S26, 2001.

37. Turker, M. S. Gene silencing in mammalian cells and the spread of DNA methylation. Oncogene, *21:* 5388–5393, 2002.

38. Laird, P. W., Jackson-Grusby, L., Fazeli, A., Dickinson, S. L., Jung, W. E., Li, E., Weinberg, R. A., and Jaenisch, R. Suppression of intestinal neoplasia by DNA hypomethylation. Cell, *81:* 197–205, 1995.

39. Eads, C. A., Nickel, A. E., and Laird, P. W. Complete genetic suppression of polyp formation and reduction of CpG-island hypermethylation in Apc(Min/+) Dnmt1-hypomorphic mice. Cancer Res., *62:* 1296–1299, 2002.

40. Eden, A., Gaudet, F., Waghmare, A., and Jaenisch, R. Chromosomal instability and tumors promoted by DNA hypomethylation. Science (Wash. DC), *300:* 455, 2003.

41. Gaudet, F., Hodgson, J. G., Eden, A., Jackson-Grusby, L., Dausman, J., Gray, J. W., Leonhardt, H., and Jaenisch, R. Induction of tumors in mice by genomic hypomethylation. Science (Wash. DC), *300:* 489–492, 2003.

42. Tsubaki, J., Choi, W. K., Ingermann, A. R., Twigg, S. M., Kim, H. S., Rosenfeld, R. G., and Oh, Y. Effects of sodium butyrate on expression of members of the IGF-binding protein superfamily in human mammary epithelial cells. J. Endocrinol., *169:* 97–110, 2001.